Investigation of the Flexural Fatigue Behavior of Stone-Faced Cork Agglomerate Sandwich Composite

Ilaria Andreazza

Instituto Superior Técnico, Universidade de Lisboa, Portugal
Università degli Studi di Padova, Italy

Date
September 2017

Keywords
Fatigue test
Damage
Sandwich
Asymmetric
Stone
Cork

Abstract

The constant quest for enhancement of the cost-performance relationship of materials is also active in the architecture field. A new concept of cladding has been invented since a decade, with the aim of maintaining the much-appreciated look of natural stone, and at the same time increasing its toughness, safety, and diminishing its specific weight. This has been possible backing a stone veneer with lighter and more resilient materials such as honeycomb or, in the present case, cork agglomerate. Although such claddings do not have a structural role, their characterization in fatigue is needed because throughout their life they will be loaded with a force variable in time coming mainly from the wind.

In this thesis, two cyclic tests have been chosen on the basis of a literature research, and carried on. The material used is made of a layer of limestone and a layer of reinforced-cork agglomerate; the reinforcement is done with glass fibers on both sides. Two configurations, L1C1 and L2C1, using limestones having different modulus of elasticity and porosity, have been manufactured and tested. The four-point bending tests had a load ratio of 0.1 and maximum load taken as a percentage of the maximum static load, i.e. from 0.70 and 0.85 of the static load for configuration named L1C1, and from 0.40 to 0.70 of the static load for configuration L2C1.

A continuous test was carried out up to 500'000 cycles or up to failure of the material, and a test with resting time after each block of cycles was used to evaluate the influence of the viscoelastic recovery of the cork.

It has been possible to evaluate the validity of the test, the occurrence or not of fatigue on the materials composing the layers, and to give a qualitative indication of the behavior of the material in service. There has been observation of different failure modes for the two configurations, and for the same configuration tested with and without stops. The failure modes vary according to the maximum load; stone indentation was always observed in the composite with the weakest stone, fiber breakage was observed for the first time on the other configuration. The tests with resting time showed a dramatic increase in lifetime compared to the lifetime of continuous tests, and were used to confirm the occurrence of permanent damage in the cork layer.

The absence in the literature of research on the fatigue of asymmetric sandwich composites makes the present work innovative in the field.

1. Introduction

A large amount of literature is present nowadays in the field of mechanics of composite materials, with comprehensive references on the study of fatigue in fiber-reinforced plastics (Harris 2003) and in sandwich structures (Daniel et al. 2010; Carlsson & Kardomateas 2011; Allen 1969), for example. Unlike for crystalline materials, though, composite fail during fatigue not because of the propagation of a single crack, but they rather accumulate damage in a general fashion (Talreja 2008). Therefore, it has not yet been possible to identify and develop a unique model to predict the fatigue life of a class of composites, because of the too many variables involved in the damage accumulation.

The composite material object of this paper (Figure 1.1) aims at replacing natural stone in all the applications where the latter is used because, besides retaining the look of a stone

cladding, it brings advantages in terms of cost, design, safety, and stability. These advantages are a direct consequence of its lower weight compared to natural stone. Its structure comprises of a first stone layer, a layer of glass fiber reinforced-resin (GFRE), a cork agglomerate layer, and a last layer of GFRE.

Figure 1.1 Exploded view of the material layers of the composite

Earlier studies (Gomes 2016; Ribeiro 2016) focused on the development of an optimized production process, and on the mechanical characterization of the material. The mechanical properties compared in order to find the best compromise between production-cost and performance, were the bending stiffness and the flexural strength.

An additional study was conducted (Correia 2016), which focused instead on the development and execution of a test to investigate the fatigue resistance of the composite. The test developed used a mixed control system: both extreme displacements and maximum force were imposed on the machine. During each cycle the specimen must reach the maximum force previously imposed, while the minimum force fluctuates, keeping the extremes of deformation constant. In doing so, the problems encountered in pure load control and pure strain control were overcome. Respectively, in pure load control the cork viscoelasticity led to excessive deformation amplitudes of the specimen, which could be harmful for the testing machine, while in pure strain an excessive decrease of the maximum load (due to mechanisms of stiffness reduction) never led the specimen to failure. The fatigue test was organized in blocks of 10^5 cycles, with the maximum load increasing of 10% of the monotonic tensile load during each block. The experiments conducted did show that there was a temperature dependence on the number of cycles at failure, as well as a mean-stress dependence; however, it is still not known which mechanism act to initiate and propagate the damage until failure. It was the purpose of this research to try to discover the causes that lead to fatigue failure of the present composite, in prospect of a future use of the material in environments subject to cyclic forces. In order to attain it, the previously developed test was of no use, and another one had to be developed prior to testing.

The challenge of the present work resides in the fact that no literature exists in the topic of fatigue behavior of cork or of cork agglomerates, if not for observation of macroscopical behavior (Reis & Silva 2009). Moreover, the asymmetrical geometry of the assembly makes it incorrect to apply the simplifications that have been used in the study of symmetrical composites.

In summary, the work will have two main objectives: first, a cyclic fatigue test is going to be designed for this new material. The parameters chosen (e.g. control mode, stress state, maximum load) don't necessarily come from stress states encountered in application of a real part, but rather relate to materials properties. In the second part, the specimens are going to be tested and the failure modes evaluated through optical, and mechanical methods, for the two composites configurations (two types of limestones and one cork type).

1.1 Design of a fatigue test

A variety of tests is possible, because of the large number of parameters characterizing the test: amplitude control, frequency, load ratio, loading direction. To date, there is no specification or international standard to test cyclic fatigue resistance of asymmetric sandwich composites. The closest resource found on the literature was the report by (S. Kneezel & J. Scheffler 2014), which followed the ASTM test by the same authors in (Scheffler et al. 2007).

Unlike in metals, in sandwich composites non-catastrophic damage events can occur throughout the stressed volume; therefore, the definition of failure is particularly difficult. The occurrence of one of this damage events may itself define the failure point. Besides traditional fracture, stiffness loss, and visual appearance have been used as failure criteria. *Compliance change* was used e.g. by (Hossain & Shivakumar 2014) in defining different types of failure according to the progression of damage; stiffness degradation was also used by (El Mahi et al. 2004) and many others in the literature, to estimate damage and model fatigue life in laminate composites. (Shafiq & Quispitupa 2006) used as damage criterion the acoustic emission amplitude and energy levels, which correspond to the occurrence of a certain damage event.

From the many factors related to fatigue testing, it appears that there are three prime issues in the choice of any fatigue program (Harris 2003). These are:

- the failure criteria to be applied (e.g. fracture, stiffness loss),
- the stress state to be applied (e.g. multi-axial, uniaxial),
- the control mode to be applied (e.g. load, displacement).

2. Materials and Methods

2.1 Materials

The studied composite material is made by a limestone backed by a glass-fabric reinforced cork sandwich. By varying the type of limestone only, two configurations were obtained, and named L1C1 and L2C1. The mechanical characteristics of the various layer will be hereafter presented, as given by the materials producers.

Two different Portuguese limestones were selected to form the stone layer of the composite material: *Branco do mar* (L1, white limestone) and *Vidraço de Ataíja azul* (L2, blue/grey limestone). The stones have similar mineral compositions, but different physical and mechanical properties, particularly due to the difference in porosity value (Table 2.1). Macroscopic analysis was performed as a general characterization of the stone structure; examinations at low magnifications were made with a common camera. Specimens examination at higher magnification were performed with the digital microscope Dino-Lite AM7515MZT.

The cork agglomerate was provided by Amorim Cork Composites. Its mechanical and physical properties are shown in Table 2.2. It is made of the agglomeration of small cork particles, whose binder is polyurethane.

Resin impregnated biaxial woven fabrics stiffen the cork layer (above and below it). The fabrics in the two layers have different grammage, being the one in contact with the stone of higher grammage in order to permit a smoother Young's modulus gradient. Their mechanical properties are given in Table 2.3.

Once the stone has the needed length and width, the production of the stone-cork composite can take place: stones are dried prior to the placement of a layer of resin-impregnated glass cloth, unless the stone is too big to fit in the drying oven. The glass fabric is impregnated of resin with the aid of spatulas, in order to have homogeneous coverage and eliminate most of the bubbles. The cork layer and the last layer of resin-impregnated cloth follow in order, and at last a polyethylene sheet prevents adherence of the resin with the plate of the hot press. The composite is then placed in a hot press where curing of the resin occurs, and later post-cured, as prescribed by the resin manufacturers. Post-cure allows for alleviation of thermal stresses, due to mass diffusion and reduction of free volume around the polymeric chains, which results is higher transition temperature, flexural resistance and higher deflection at break. The final process comprehends the lowering of the stone layer to a thickness of about 5 mm, and the cutting of the plate in specimens of the final dimensions (300 mm x 50 mm).

Table 2.1 Mechanical properties of the used limestones

	Branco do Mar (L1)		Vidraço Azul (L2)	
Compression strength	51,97	MPa	161,8	MPa
Flexural strength	7,5	MPa	10,3	MPa
Apparent density	2280	Kg/m3	2680	Kg/m3
Water absorption	6.2	%	0.4	%
Open porosity	13.3	%	0.9	%

Table 2.2 Cork mechanical properties as provided by the manufacturers

	Cork	
Density	200	Kg/m^3
Compressive Strength	0,5	MPa
Compressive Modulus	6	MPa
Tensile Strength	0,7	MPa
Shear Strength	0,9	MPa
Shear Modulus	5,9	MPa

Table 2.3 Mechanical properties of the glass fabrics

	Biaxial fabric 1	*Biaxial fabric 2*	
Weave	Plain	Plain	
Areal density	612	290	g/m^2
Filament diameter	12 to 15	8,9 to 10,2	µm
Tensile strength	1900 to 2400	1900 to 2400	MPa
Tensile Modulus	69 to 76	69 to 76	GPa
Elongation at break	3,5 to 4	3,5 to 4	%
Thickness	0,23077	0,29	mm

2.2 Methods

The static and fatigue testing was performed using the same geometry, with the stone layer on the compressive side. The chosen test is a third-point 4-pt-bending test; the measures of the outer span l_1, inner span l_2, and specimen width, b, are 250, 83.3, and 50 mm respectively. The testing machine for both tests is the servo-hydraulic Instron 8800, with load cell of 100 kN. The cylindrical rollers have a radius of 20 mm.

Static tests were carried out to determine the failure load (F_{UF}) of the materials, which will then be used to define minimum and maximum force (F_{MIN}, F_{MAX}) of the fatigue cycles. The tests are conducted at constant velocity of 5 mm/min.

Continuous fatigues tests were performed in load control, at a frequency of 2.7 Hz for L1C1 and of 4 Hz for L2C1, sinusoidal waveform, load ratio R = 0.1, and maximum load

chosen as a percentage of the static failure load. Due to time limits, all the tests were stopped at 500'000 cycles, or when catastrophic failure occurred. The fatigue test variables (R, F_{MIN}, F_{MAX}, F_A) are dependent by the relations $R = F_{MIN}/F_{MAX}$ and $F_A = (F_{MAX} - F_{MIN})/2$. Therefore, only two variables need to be arbitrarily chosen.

Interrupted fatigue tests, with a resting time of 24 hours between blocks were conducted for L2C1 at load percentages of 45, 50, 55, 60%. The number of cycles in a block is equal to 70% of the failure cycles (N_f) in the continuous tests.

Several parameters were calculated from the raw data of the testing machine:

- **Relative stiffness D_{rel}.** Since the load-deflection curve is not linear, it is necessary to define two force values between which to calculate the slope, which is equivalent to the tangent stiffness of the two points. The extremes were decided, for the two materials, according to where the linear part of the curve is located. In L1C1 it is calculated between 300 - 600 N, in L2C1 between 600 - 900 N.
- **Absolute stiffness D_{abs}**. When the number of cycles increases, the material accommodates a deformation which is not instantaneously recovered, and which is not taken into account in the calculation of D_{rel}. Therefore, D_{abs} has been introduced to have a unique parameter where both the slope of the curve and the accumulated deformation are included.
- **Accumulated deformation d_{acc}**. It is the deformation not recovered at force F_1, and equal to the difference between the position of the n*th* cycle and of the first cycle at F_1: $d_{acc}^n = d_n(F_1) - d_1(F_1)$.
- **Dissipated energy**. It is quantified by the area inside the hysteresis loop. In this case, the integration has been done using the trapezoidal approximation:

$$A_j = \sum_{i=1}^{n-1} (F_i + F_{i+1}) \cdot (d_{i+1} - d_i) \cdot \frac{1}{2},$$

where A_j is the area of the j*th* cycle, and n the number of data per cycle.

- **Cumulative dissipated energy**. It is the cumulative sum of the energy dissipated in every cycle. Since the testing machine only saves data of a limited number of cycles, it is assumed that the energy absorbed in the cycles where no data are available is the average between the energy of the previous and next known cycles.

3. Results

As is visible in Figure 3.1,due to the porous structure of L1, there is a visible boundary between the zone where resin was absorbed and where there is no resin; in this thin layer, all pores are filled with the resin, and the grains become indistinguishable. L2 has a compact structure, with no visible pores nor layer of resin absorption.

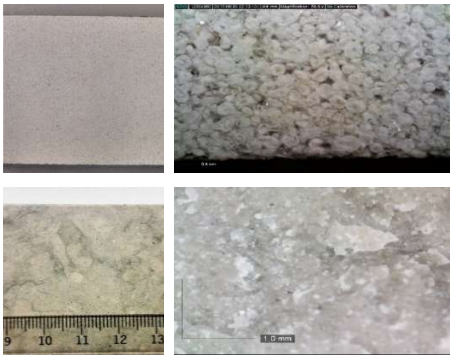

Figure 3.1 Macroscopic (left) and microscopic (right) examination of the limestones L1 (top) and L2 (bottom).

The results of the static tests are shown in Figure 3.2; the red lines indicate the limits between which stiffness is calculated in the cyclic tests.

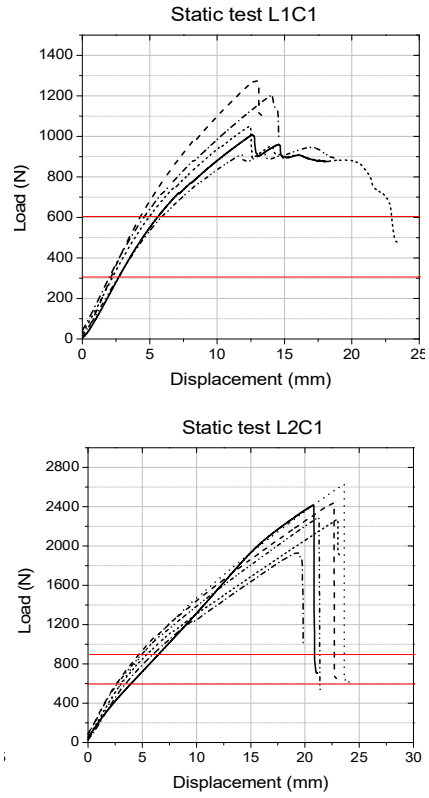

Figure 3.2 Load-displacement curves for the static tests L1C1 and L2C1

The unevenness of specimen thickness, t, influences the failure load of L1C1, which can be described by:

$$t = 0.0026\, F_{UF} + 17.635\ .$$

As for L2C1, there has been no identified dependence $F_{UF}(t)$ both because a) the standard deviations of the thickness measurements on the same specimen are lower than in L1C1, and b) the variability of the average of the thicknesses is low.

It has been therefore concluded that F_{UF} of L2C1 can be taken as the average of the failure loads: 2409 N.

The maximum force (F_{MAX}) of the fatigue cycle is always calculated as a percentage of the static failure load. The results of the two materials tested are summarized in Figure 3.3.

In all cases, L1C1 failure occurred due to crushing of the stone layer; L1C2 instead showed different modes of failure according to the applied load percentage (Figure 3.4):

- For $F_{MAX} > 60\%\ F_{UF}$ failure occurred due to indentation of the limestone, as was in L1C1.
- For $45\%\ F_{UF} < F_{MAX} < 55\%\ F_{UF}$, we observed a change in failure mode: failure occurred because of breakage of the lower layer fibers, and crack propagation in the cork layer in the direction of maximum shear stress.
- For $F_{MAX} < 45\%\ F_{UF}$, no fracture was observed.

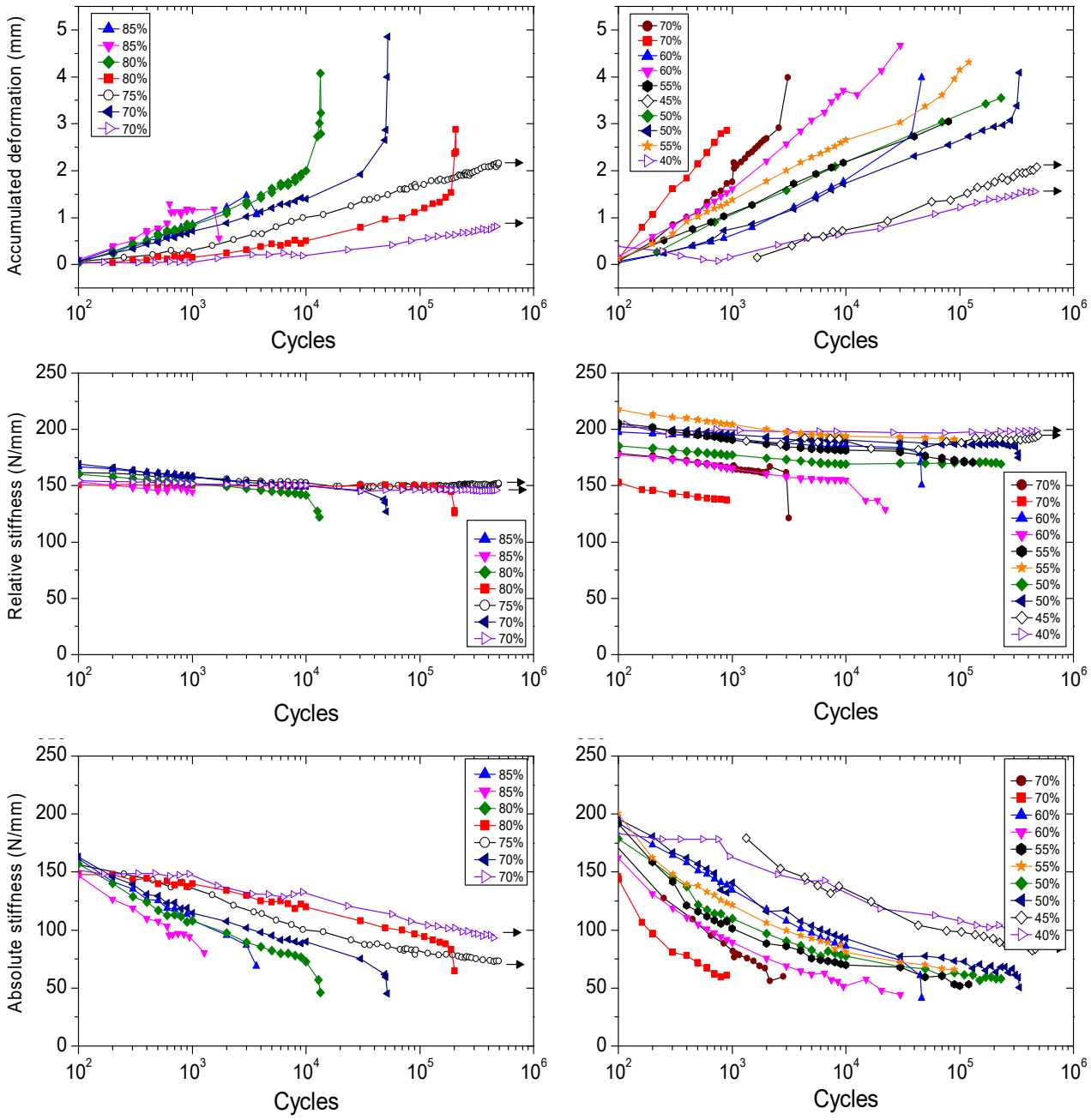

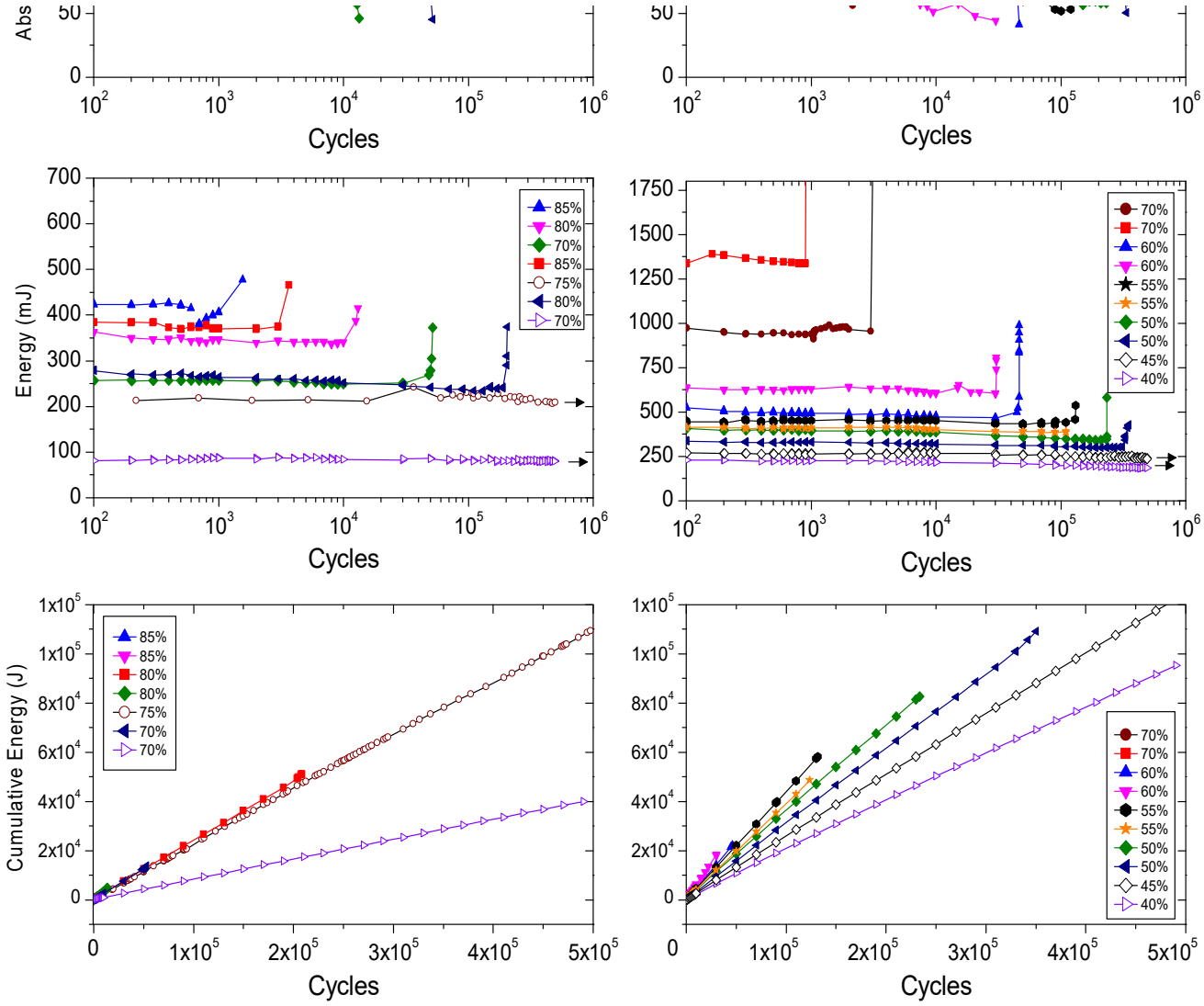

Figure 3.3 Trend of the quantities 1) accumulated deformation, 2) relative stiffness, 3) absolute stiffness, 4) dissipated energy, and 5) cumulative energy along the cycles for L1C1 and L2C1

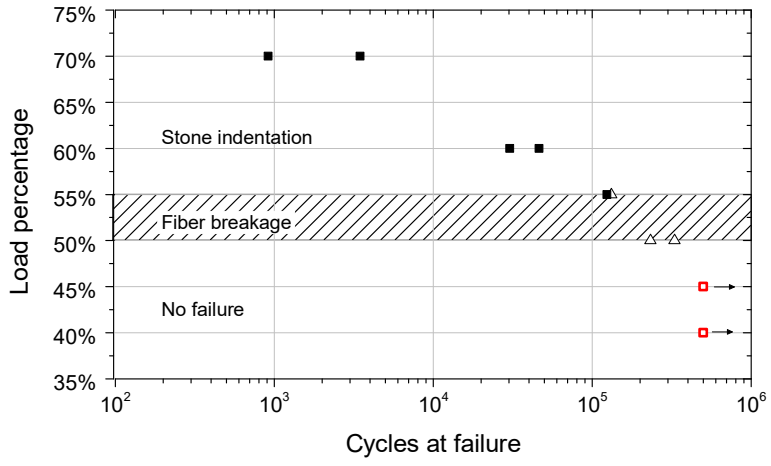

Figure 3.4 Failure mode map for L2C1

Figure 3.5 Macro-cracks on the cork layer on the fatigue tests with resting time

Tests with resting time were carried out for L1C1, at the load percentages already mentioned; only the results of 55% will be reported here, the others showing similar trends. The test at 45% did not show any sign of failure after two blocks of 500'000 cycles. The tests at 55, 60, and 60% instead failed showing a common feature: multiple macrocracks at 45° orientation on the cork layer located at the right- and at the left-side of the left and right roller, respectively (Figure 3.5). The resulting number of cycle at failure for the various percentages are given in

Table 3.1.

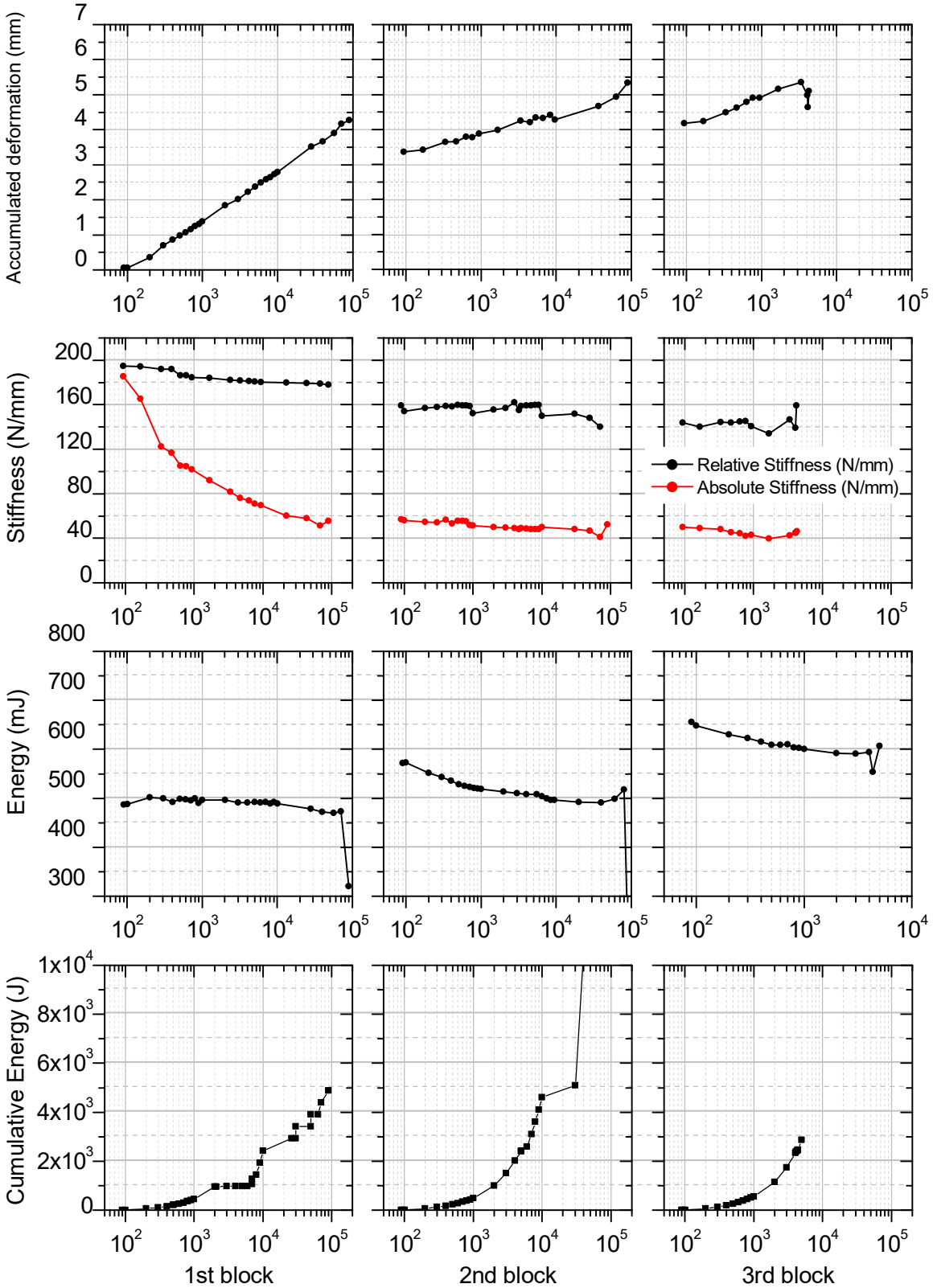

Figure 3.6 Trend of the quantities 1) accumulated deformation, 2) relative stiffness & absolute stiffness, 3) dissipated energy, and 4) cumulative energy along the cycles for L1C1; tests with resting time of 24 hours between blocks.

Table 3.1 Comparison of the number of cycles at failure (N_f) of tests with and without resting time

Load percentage	*N_f continuous tests*	*N_f tests with resting time*	*Life increase*
55	127'000	185'000	145%
60	38'000	104'000	274%
65	3'600	8'000	222%

4. Discussion

4.1 Accumulated deformation

For both materials, d_{acc} shows a linear trend in logarithmic x-scale, meaning that there is a rapid increase until about 10^4 cycles, after which, unless the material fails shortly after, it stabilizes to a plateau. Curves tend to have higher stabilization deformation for increased load percentages, although for L1C1 a curve at (theoretical) load percentage of 80% has lower d_{acc} than the one at 70%. Material L2C1 shows a more regular behavior, with linear curves and approximately decreasing slope for decreasing load percentage.

The fact that all curves for the two materials have a linear trend, or logarithmic trend in linear scale, means that there always is an initial period during which the material loses part of its stiffness. The number of cycles until stabilization is, for both materials, 10'000 cycles. As shown by the test with stops, the loss in stiffness is permanent, and could be associated to a damage in the cork layer.

Overall, the d_{acc} at failure for L2C1 is set at higher values than for the other configuration (3 to 4 mm versus 1 to 3 mm); the cause could be found in the higher compressive resistance of the stone L2. The increase in d_{acc} is due to the viscoelastic nature of the cork layer; cork is microscopically made of cells with elastic walls which corrugate under stress. When stress is released, the corrugation is also recovered, but recovery has a time delay. Since the frequency of the cyclic loading is higher than the time needed for recovery, cork does not recover all its deformation, and the remaining is accounted for in d_{acc}.

The trend of d_{acc} at failure in L1C1 seems to be inferring that lower load percentages have higher accumulated deflection at failure, although the penetration of the rollers on the cork is not considered. The same happens for L2C1, although the data are more scattered.

4.2 Relative & absolute stiffness

L1C1 always shows an initial decrease until stabilization at a constant value, which is maintained until before failure. Materials showing infinite life have a curve with slope zero and similar value of relative stiffness (145-150 N/mm): this is a confirmation of the homogeneity of the stone composition. Failure might have different causes: at low cycles, it is caused by the impact of the rim on the stone, at high cycles by the deflection and a probable fatigue effect.

The initial decrease of D_{rel} (until 10^3 cycles) is shown both for L1C1 and L2C1, and can be attributed to a damage of the cork layer. Instead, a faster decrease in stiffness for load percentages above 60 in L2C1 could indicate another damage mechanism, probably on the stone, since it is the stone that fails due to crushing. At higher loads the damage happens faster; before the 100th cycles shown on the graphs, the cork already lost its initial stiffness, increasing the bending deflection. Higher deflections at constant frequency, and slow recovery of deformation induce the composite to be loaded abruptly, until the repeated impact of the loading pin on the stone generates failure.

4.3 Energy

The graphs of dissipated energy per cycle show whether there is or not a variation in the shape of the hysteretic loops, which in turn is an indication of occurrence of energy dissipating processes. Specimens with the highest absorbed energy per cycle fail at the lowest number of cycles, for both materials. L2C1 graph indicates that the energy absorbed per cycle increases for higher maximum loads, as it is expected, because they are associated to increasing values of F_{MAX}. Moreover, in all cases the plateau energy value is constant until failure, following the same trend as the relative stiffness. This confirms that there are not additional relevant damage processes before failure.

The curves for cumulative energy showed a predictable trend: looking at L2C1, specimens tested at lower load percentages absorb less energy per cycles, therefore accumulate energy more slowly, and their slope is lower than for specimens which fail sooner. Overall, the cumulated energy at break is not constant, but higher for specimens that last longer. This means that the mechanisms inducing energy dissipation in infinite-life specimens do not degrade the properties of the material, because of an equilibrium between energy dissipation – probably in the form of heat – and thermal exchange with the environment.

4.4 Fatigue tests with resting time

The most evident results of this kind of tests are:

The specimens last longer than in continuous tests, for equal load percentages (

- Table 3.1).
- There is permanent cork damage, as can be deduced by a) the relative stiffness not going back to the initial value, and b) the d_{acc} rapidly reassuming the value it had before the resting time.
- The cork suffers from fatigue. More precisely, it is the resin used as adhesive of the granules that fails due to cyclic effect, and the mechanical resistance of the cork is degraded

The motivation underlying the first point is not clear. It is assumed that, besides the permanent damage on the cork suffered in the first cycles, there is a damage component which is recovered during the resting time, probably related to the architecture of the cork cells. Regarding the second point, the resin is the weakest link of the agglomerate, the cell walls do not fail. This is in agreement with previous tensile and shear tests done on the cork only.

The graphs of absorbed energy along cycles are also peculiar: for 55, 60, and 65 % the energy dissipated in blocks other than the first has a high initial value, then decreases. The resting induces recovery of some viscoelastic deformations, recovery which is lost again at the beginning of each new block. It is unclear whether the recovery is in the cork, in the stone, or in the fibers.

4.5 Failures

Failures at low cycles in both materials are believed to be caused by the impact of the loading pin on the stone, and not by the the stone deflection. This is because specimens fail at a maximum deflection much lower than that obtained in the static tests.

For L1C1 specimens failing at high cycles, the deflection reached is similar to that reached in the static tests, although still slightly lower; nevertheless, test velocity might also influence F_{UF} and d_{UF}. In this cases, the failure occurs not for impact but because of overcoming the maximum deflection at break.

For L2C1, the situation is different; although for load percentages of 60 and above, the impact of the loading pin causes failure, at 55%, the failure mode shifts. Here, due to the permanent deformation increasing slowly, the stone does not suffer from the previous effect, and the life increases considerably (from 10^4 to 10^5 cycles). This additional cycles therefore damage the layer which sustains the second highest stresses: the bottom glass-fiber layer. Damage is initiated where defects are: fabric cross-overs, undulations, or bubbles in the resin. This type of fracture is not present in L1C1 because the stone crushing occurs at lower stresses, nor it is visible in L2C1 above 55%.

Interestingly, failure of the lower fibers did not occur in the specimens tested with resting time. Here, the specimens showed typical shear failure modes of symmetric sandwich composites tested in static or fatigue (Zenkert & Burman 2009).

5. Conclusions

Two material configurations have been manufactured, L1C1 and L2C1, differing only by the type of limestone used in the upper layer. The measurements of thickness and the static flexural tests showed that the load at failure of L1C1 varies linearly with the composite thickness, while load at failure of L2C1 does not show correlation with thickness.

The limestone in configuration L1C1 determines the cyclic failure of the composite, being it always due to stone crushing; it is believed that failure at low cycles is due to the impact of the loading pin, while at high cycles it is due to overcoming the limit deflection of the composite; infinite life occurs for $F_{MAX} < 70\%$.

For configuration L2C1, failure at high cycles also happens caused by the impact of the loading pin; for a $F_{MAX} < 55\%$ though, the failure mode shifts to lower fiber breakage, and below 45% the composite can sustain infinite cycles. In order to have an increased fatigue resistance, it is convenient to improve the quality of the lower fiber layer, namely its grammage and geometry.

The resting time between cycles has a life-increasing effect, also to be attributed to the cork because of its viscoelasticity. It is therefore not possible to apply a damage predicting law in the form of a Miner's law. This adds further complication where one wants to model the composite behavior, but in sight of a future application where the composite component is subject to variable loads coming from the wind, the component life is positively affected. In tests with resting time, the failure occurred for cork shearing, demonstrating another possible mode of failure, for L2C1.

Future studies should be conducted regarding:

- Determination of the strains on each material layer, as well as the location of the neutral line with extensometers or VIC analysis; determination of the rock elastic modulus with, for example, the resonance method.
- Performance of fatigue tests in position control, and at constant velocity instead of constant frequency.
- Performance of fatigue tests with randomly variable loads and with $R < 1$, simulating the effect of the wind.
- Influence of the change of lower layer glass fibers on the fatigue behavior.
- Performance of fatigue tests on real components, in order to account for the effect of the fixing system on fatigue.

6. References

Allen, H.G., 1969. *Analysis and Design of Structural Sandwich Panels* 1st ed., Oxford: Pergamon Press.

Carlsson, L.A. & Kardomateas, G.A., 2011. *Structural and Failure Mechanics of Sandwich Composites*, Dordrecht: Springer Netherlands.

Correia, F.L., 2016. *Fatigue analysis of an asymmetric composite structure composed of dissimilar materials - thesis*. Istituto Superior Tecnico.

Daniel, I.M., Gdoutos, E.E. & Rajapakse, Y.D.S., 2010. *Major Accomplishments in Composite Materials and Sandwich Structures*, Dordrecht: Springer Netherlands.

Gomes, G., 2016. *Characterization and optimization of the production process of sandwich composite structures*. Istituto Superior Técnico.

Harris, B., 2003. *Fatigue in composites: science and technology of the fatigue response of fibre-reinforced plastics*, Woodhead Publishing.

Hossain, M.M. & Shivakumar, K., 2014. Flexural fatigue failures and lives of Eco-Core sandwich beams. *Materials and Design*, 55, pp.830–836.

El Mahi, A. et al., 2004. Modelling the flexural behaviour of sandwich composite materials under cyclic fatigue. *Materials and Design*, 25(3), pp.199–208.

Reis, R.L. & Silva, A., 2009. Mechanical behavior of sandwich structures using natural cork agglomerates as core materials. *Journal of Sandwich Structures and Materials*, 11(6), pp.487–500.

Ribeiro, J., 2016. Avaliação do comportamento mecânico de estruturas compósitas tipo sanduíche de baixo peso específico utilizando materiais naturais. , p.83.

S. Kneezel, D. & J. Scheffler, M., 2014. Stone-Faced Aluminum Honeycomb Composites — Quality Control and Testing. In *28th RCI international convention and trade show*. pp. 155–167.

Scheffler, M.J. et al., 2007. Testing of Composite Stone Faced Aluminum Honeycomb Panels. *Journal of ASTM International*, 4(7), p.100854.

Shafiq, B. & Quispitupa, A., 2006. Fatigue characteristics of foam core sandwich composites. *International Journal of Fatigue*, 28(2), pp.96–102.

Talreja, R., 2008. Damage and fatigue in composites - A personal account. *Composites Science and Technology*, 68(13), pp.2585–2591.

Zenkert, D. & Burman, M., 2009. Tension, compression and shear fatigue of a closed cell polymer foam. *Composites Science and Technology*, 69(6), pp.785–792.